

PERIODICO di MINERALOGIA
established in 1930

*An International Journal of
MINERALOGY, CRYSTALLOGRAPHY, GEOCHEMISTRY,
ORE DEPOSITS, PETROLOGY, VOLCANOLOGY
and applied topics on Environment, Archaeometry and Cultural Heritage*

Analysis of the plasters of some relevant chapels of the Sacro Monte (Sacred Mountain) of Varallo Sesia, Piedmont, Italy

Jean-Marc Tulliani^{1,*}, Paola Palmero¹, Riccardo Sandrone² and Elena Defilippis³

¹Dept. of Applied Science and Technology, Politecnico di Torino, INSTM R.U. PoliTO-LINCE Lab,
Corso Duca degli Abruzzi 24, 10129 Torino, Italy

²Dept. of Environment, Land and Infrastructure Engineering, Politecnico di Torino,
Corso Duca degli Abruzzi 24, 10129 Torino (Italy); +390115647646; +390115647699;

³Piazza della Basilica, Località Sacro Monte, 13019 Varallo (VC) (Italy); +39016353938;

*Corresponding author: jeanmarc.tulliani@polito.it

Abstract

Varallo Sacred Mountain was realized at the end of the fifteenth century on initiative of the Franciscan Father Bernardino Caimi as a place of prayer, meditation and evocation of the Christian faith and has been included in the UNESCO World Heritage List since 2003. Some of its buildings show at the moment manifold maintenance, conservation and restoration problems. Therefore, in the frame of a detailed program of interventions, a research co-operation has been launched, aiming at singling out the existent materials and, as much as possible, their working techniques. In particular, this paper deals with the investigations carried out by means of X-Ray diffraction, scanning electron microscopy observations coupled with elemental analysis, as well as optical microscopy on the plasters of three relevant parts of the “*Sacro Monte*”, precisely the complex of the Crucifixion, the Square of the Courts, the chapel of Christ’s Transfiguration on Mount Tabor. Results from the investigated samples indicated that in all cases aerial binders were used together with local aggregates from the Sesia River. Some particular compositions were found in the three buildings, probably to obtain specific aesthetic effects. Several finishing layers used for the outside walls of the Chapel of Crucifixion were made of mixed gypsum-lime mortars, probably for aesthetical reasons, while typical lime mortars were found together with dolomitic ones in the Square of the Courts and in the Mount Tabor chapels. Finally, because of the use of dolomitic limes, hydromagnesite was also evidenced in some mortars.

Key words: Plasters; microstructural characterization; X-Ray diffraction; SEM observations; mineralogical-petrographical observations.

Introduction and research aims

The “*Sacro Monte*” of Varallo Sesia, Piedmont, Italy (Figure 1) was conceived at the end of XV Century, on initiative of Franciscan Father Bernardino Caimi, keeper of the Holy Sepulchre. Once returned to his native soil, he devised the ambitious plan to build a copy of the Holy Land, witness of the earthly life of Christ, in close agreement with the Franciscan spirituality devoted to recover the piety of Early Christianity.

Chapels in which frescos and sculptures in wood and terracotta are dedicated to the most relevant moments of Christ’s life, as a place of pilgrimage for people unable to go to Palestine, were therefore conceived and started to be built.

The “*Sacro Monte di Varallo*” has been included in the UNESCO World Heritage List since 2003 and some of its buildings show

manifold maintenance, conservation and restoration problems. This study represents the first step of a detailed program of investigations, aimed at singling out the existent materials and, as much as possible, the ancient building techniques; studying and interpreting the most frequent decay pathologies in progress and assessing a restoration project based on a background knowledge of ancient materials. In particular, this paper deals with the investigations carried out on the plasters of three relevant parts of the “*Sacro Monte*”, precisely the complex of the Crucifixion, the Square of the Courts, the chapel of Christ’s Transfiguration on Mount Tabor.

The Chapels of the Calvary

The sites of Nazareth, Bethlehem, Gethsemane and Zion were already present in the first “*Sacro Monte*”, as described by a Franciscan guide in

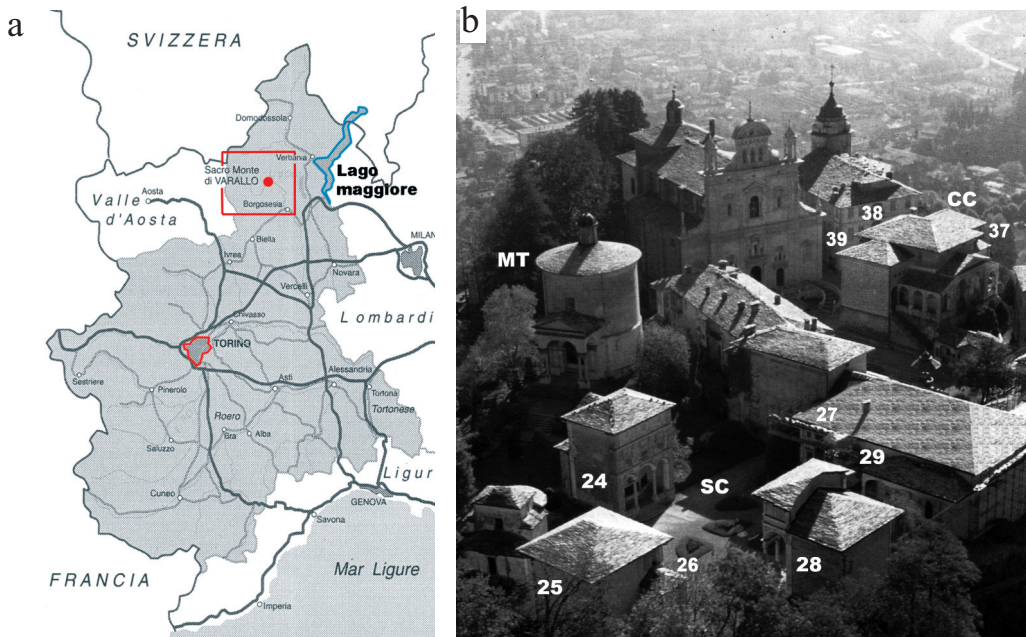


Figure 1. Position of Sacro Monte of Varallo with respect to North-Western Italy a); Partial aerial view of Sacred Mountain of Varallo b) (Stefani Perrone, 1994). SC = Square of the Courts; MT = Mount Tabor; CC = Chapel of the Crucifixion.

1514. In 1520, on the top of the Calvary hill, the Chapel of the Crucifixion (now Chapel no. 38) which represents the artistic and thematic heart of the "Sacro Monte", i.e. the drama of Christ's Passion, was under construction. It was probably made by following a project of Gaudenzio Ferrari and was completed with frescoes and sculptures within 1521. The construction of the adjacent chapel of the Nailing to the Cross (now Chapel no. 37) was promoted by the Bishop Carlo Bascapé in 1603 to reorganise the Sacred Mountain in agreement with the provisions of the Council of Trent. It was probably designed by Giovanni d'Enrico and Bartolomeo Ravelli at the beginning of the XVII Century, but it was built only in the years 1630s and decorated with statues made by Giovanni d'Enrico and Giacomo Ferro and painted inside by Melchiorre Gherardini. On the other side of the Crucifixion chapel, the chapel of the Deposition from the Cross (now Chapel no. 39) was also built and decorated during the years 1630s by the same architects and artists.

The complex of the Crucifixion made of these three adjacent chapels maintained its original structure up to the end of the XVIII Century. An additional floor was added to the central chapel of the Crucifixion in the first half of the XIX Century, and in 1851-52 Giacomo Geniani placed a large loggia in front of the western façade, crowned by a tympanum. The last relevant change was the construction of an arched portico based on pillars, surmounted by a small loggia with stone columns, in the middle of the XX Century.

The Square of the Courts

This Square is delimited by various chapels, each of them representing a scene of Christ's life into a Court: that of Anna (chapel no. 24) and of Caifa (chapel no. 25), the chapel remembering St Peter's repentance (chapel no. 26), the first time in the Pilate's palace (chapel no. 27), the Court of Erode (chapel no. 28), and finally the

last time in the Pilate's palace (chapel no. 29). Chapel no. 24 was built in the XVIII Century, but all the other chapels were built in the first thirty years of the XVII Century following the projects of Giovanni d'Enrico and Bartolomeo Ravelli, whose work was the slow evolution of the original ideas of Galeazzo Alessi (1565-1569).

The chapel of Christ's Transfiguration on Mount Tabor

The chapel of Christ's Transfiguration on Mount Tabor is a large and monumental building perfectly integrated with the surrounding rocks. Designed by Alessi (1565-1569), it was constructed between the end of XVI Century and the middle of the XVII Century on the remains of a previous chapel. The inside was decorated with frescos made in 1665 by the brothers Giovanni Stefano and Giuseppe Danedi, also called "Montaldi da Caravaggio", and by many statues made by Gaudenzio Soldo da Camasco in 1670-71.

Experimental section

Materials

The investigated site is characterized by a large complexity of construction steps, spread over a relevant period of time. Starting from rigorous historical studies based on archives and iconographic documents (AA.VV., 1514, Galloni, 1914, Stefani Perrone, 1984), an extensive in-situ analysis was first performed to determine the historical constructive stratifications and the related sampling plan of the outside plasters of some chapels. Only a limited number of the many analysed samples have been considered for this paper (Table I), selected on the ground of their historical and scientific relevance. The samples were identified by an alpha-numerical code, in which the letters CC, SC and MT, representing the sampling location from Complex of the Crucifixion,

Table I. Location and description of the plaster samples.

Sample	Sampling point	Description
CC1	Chapel of the Crucifixion (Chapel no. 38)	Sampled on a wall of Gaudenzio Ferrari's period, located inside the eastern loggia
CC2	Chapel of the Crucifixion (Chapel no. 38)	Sampled on a wall of the XVII century, located inside the eastern loggia, near the edge with the previous Gaudenzio Ferrari's wall (sample CC1)
CC3	Chapel of the Crucifixion (Chapel no. 38)	Sampled on a wall probably of Gaudenzio Ferrari's period, presently inside a room at the ground floor on the western side of the Chapel
CC4	Chapel of the Crucifixion (Chapel no. 38)	Sampled on a painted cornice of Gaudenzio Ferrari's period, presently located in the western garret of the Chapel
CC5	Chapel of the Crucifixion (Chapel no. 38)	Sampled in depth on the inside wall under the easter portico at the border with Chapel n.39 (Deposition from the Cross), after removal of a super-posed plaster of the XIX Century
CC6	Chapel of the Crucifixion (Chapel no. 38)	Sampled on rounded cornice inside the boundary between the roofs of Chapels no. 37 and 38, corresponding to the extrados of Chapel no. 37
CC7	Chapel of the Crucifixion (Chapel no. 38)	Sampled on a raised wall of Chapel
CC8	Chapel of the Crucifixion (Chapel no. 38)	Sampled on a wall inside the garret of the western part (XIX Century)
CC9	Chapel of the Crucifixion (Chapel no. 38)	Sampled on the western outside wall (XIX Century)
CC10	Chapel of the Crucifixion (Chapel no. 38)	Sampled on the eastern outside wall of the loggia (XIX-XX Century)
SC1	Square of the Courts, (Chapel no. 24)	Sampled on the western outside wall over a loggia facing the square (probably XVIII Century)
SC2	Square of the Courts, (Chapel no. 25)	Sampled on the western wall, inside the present lift-shaft, at about 1 m from the floor. It was an outside wall up to few years ago. (probably XVII Century)
SC3	Square of the Courts, (Chapel no. 28)	Sampled on the northern outside wall, on high, over an elevation probably dated in XIX Century
SC4	Square of the Courts, (Chapel no. 28)	Sampled on the northern outside wall, on high, under the elevation probably dated in XIX Century of Sample SC3. Sampled on the tambour of the Chapel, on high over the location of sample MT2 (probably XVII Century)
SC5	Square of the Courts, (Chapel no. 29)	Sampled on the northern outside wall (probably XVIII Century)
SC6	Square of the Courts, (Chapel no. 29)	Sampled on the northern outside wall under a loggia, directly from the surface of the stone wall, after removal of a super-posed plaster (probably XVII Century)
MT1	Chapel of Mount Tabor	Sampled on NNW wall on the tambour of the Chapel, on high over the location of sample MT2 (probably XIX Century)
MT2	Chapel of Mount Tabor	Sampled on NNW wall on the tambour of the Chapel, under the location of sample MT1 (probably XVII Century)
MT3	Chapel of Mount Tabor	Sampled on NNW wall over the skirting board (probably XVII Century)
MT4	Chapel of Mount Tabor	Sampled on NNW wall on the cornice (probably XIX Century)

Square of the Courts and Mount Tabor, respectively, are followed by an identification number.

Analytical methodologies

The morphology and texture of the plasters were investigated by using a Scanning Electron Microscope (SEM, Hitachi S2300-D), equipped with an energy dispersive X-ray spectrometer (EDS KeveX) to collect elementary semi-quantitative analytical data. To collect statistical data, a large number of data acquisitions was collected at a relatively low magnification (1000 x) of the finishing surfaces.

The plaster samples were ground and sieved first through a 600 μm -opening sieve and then the passing fraction was divided in two parts by sieving through a finer sieve. The lowest fraction (< 45 μm) is considered to be prevalently made of the binder phase (Callebaut et al, 1999), although variable amounts of finely grained aggregates could sometimes be found in this fraction. Both fractions were then finely pulverised and submitted to X-ray diffraction analysis (XRD, Philips PW 1710) in order to identify the mineral crystalline phases. It is fundamental to underline that, when present, the coloured finishing plaster layer has been separated from the mortar before crushing and sieving. Almost all samples have been analyzed, except CC4 and CC6, because of their limited size.

Simultaneous TG-DSC thermal analyses (Netzsch STA 409) were performed on about 25 mg of powdered and sieved SC4 sample to better identify some phases (specifically, magnesite, dolomite and hydromagnesite). The analysis were done under static air, with a heating rate of $10^\circ\text{C min}^{-1}$ in the temperature range 25-1000 $^\circ\text{C}$; the investigated and the reference samples were placed into alumina crucibles.

Optical microscopy of thin sections of plaster samples was used for the mineralogical-petrographical characterization of the constituents (following the NORMAL Standard

12/83). Image analysis (Image-Pro Plus 7.0 by MediaCybernetics Inc.) was also performed on images from optical microscope to determine aggregates size and quantity in volume, i.e. the ratio between aggregate and binder. Aggregates detection was done image by image, as a function of the contrast of each picture, by adjusting the grey value threshold. Once the aggregates were highlighted, the system measured the corresponding area of all the thresholded objects and then converted it into an equivalent diameter, assuming that all of them were equivalent to perfect circles. All these diameters were finally "high-passed filtered" by means of a minimum value (0.03 mm) chosen to remove the smallest objects corresponding to aggregates or parts of aggregates that were not correctly detected.

This investigation has been performed on most samples (except CC4, CC6, CC9 and SC5 due to their small size), from which a few millimetres thick slice has been firstly dry-sawn, then consolidated by a thermosetting resin at 160°C (Inesco; Cod. 000.0160), and finally a thin section has been obtained.

Experimental data and results

Chapel of the Crucifixion

XRD patterns revealed that the binder phase in most plaster samples is made of pure lime (CaCO_3), except in sample CC3 in which traces of dolomite [$\text{CaMg}(\text{CO}_3)_2$] and ferroan magnesite [$(\text{Mg,Fe})\text{CO}_3$] were detected as shown in Figure 2. In samples CC2 and CC7 also traces of gypsum ($\text{CaSO}_4 \cdot 2\text{H}_2\text{O}$) were present.

The presence of dolomite is due to the fact that the raw materials were extracted from the Mount Fenara, close to the Varallo site, known for providing a "strong" lime after thermal treatment (AA.VV., 1842). A number of studies have focused on the analysis of the carbonation of dolomitic lime mortars, which is a more complex process than the carbonation of calcitic lime

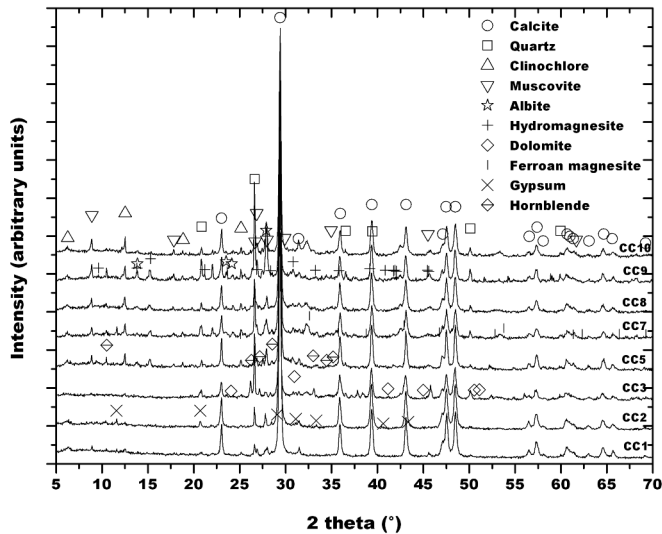


Figure 2. XRD pattern of the investigated CC plasters.

(Cultrone et al., 2008). On one hand, the reaction of portlandite $[\text{Ca}(\text{OH})_2]$ with atmospheric CO_2 leads to the formation of calcium carbonate, as in calcitic limes. On the other hand, the carbonation of brucite $[\text{Mg}(\text{OH})_2]$ results in the formation of amorphous (hydrated) Mg carbonate and/or (metastable) hydrous carbonates including hydromagnesite $[\text{Mg}_5(\text{CO}_3)_4(\text{OH})_2 \cdot 4\text{H}_2\text{O}]$, dypingite $[\text{Mg}_5(\text{CO}_3)_4(\text{OH})_2 \cdot 5\text{H}_2\text{O}]$, artinite $[\text{Mg}_2\text{CO}_3(\text{OH})_2 \cdot 3\text{H}_2\text{O}]$, nesquehonite $(\text{MgCO}_3 \cdot 3\text{H}_2\text{O})$, and lansfordite $(\text{MgCO}_3 \cdot 5\text{H}_2\text{O})$ (Cultrone et al., 2008). Formation of the thermodynamically stable magnesite (MgCO_3) is kinetically hindered: apparently, magnesite forms at high temperature, following dehydroxilation of brucite and solid state carbonation (Cultrone et al., 2008). As dolomite can not be formed after carbonation of dolomitic lime, it is highly probable that the evidenced one is a rest of unburnt dolomite.

The presence of the iron-magnesite could be due to the dedolomitization reaction of the unburnt dolomite, which reacts with portlandite, producing calcite and brucite (Galí et al., 2001).

Elemental composition analyses performed on the finishing layers by EDS have revealed the common presence of some chemical elements, besides O, such as Mg, Al, Si, Ca (mostly predominant), and Fe, which are in good agreement with XRD data collected on plasters and aggregates. In addition, Na and K were detected in samples CC2, CC3, CC5, CC6, whereas only K was detectable in samples CC1, CC4, CC7, CC8, CC9, CC10. The most relevant difference was the noticeable amount of S characterising the finishing layers and which is not in contrast with the compositional results collected on binder and aggregate of the underlying mortars (Table 2).

In addition, at higher magnifications, it was possible to observe the presence of acicular crystals (Figure 3) having the classical morphology of gypsum crystals, and predominantly made of Ca, S and O.

The presence of gypsum in the finishing layers was confirmed by submitting an almost flat surface portion of most analysed samples to XRD (Figure 4). Therefore, in most cases,

Table 2. EDS analysis results on CC samples.

Sample	Elements
CC1 finishing layer	Ca (+++), S (++) , Mg (+), Si (+), Al (+), K (+), Fe (+)
CC2 finishing layer	Ca (+++), S (++) , Mg (+), Si (+), Al (+), K (+), Na (+), Fe (tr), K (tr), Cl (tr)
CC3 finishing layer	Ca (+++), S (+), Mg (+), Si (+), Al (+), K (+), Fe (+), Na (+), P (+), Cl (+)
CC4 finishing layer	Ca (+++), Mg (++) , Si (++) , Al (+), K (+), Fe(+)
CC4 layer below finishing one	Ca (+++), Mg (+), Si (+), Al (+), S (+), K (+), Fe (+),
CC5 finishing layer	Ca (+++), Mg (++) , Si (+), S (+), Al (+), K (tr), Fe(tr), Na (tr), P (tr), Cl (tr)
CC6 finishing layer	Ca (+++), Si (++) , S (++) , Mg (+), Al (+), K (+), Na (tr), Cl (tr)
CC7 finishing layer	Ca (+++), S (++) , Si (+), Mg (tr), Al (tr), K (tr), Fe (tr), P (tr)
CC8 finishing layer	Ca (+++), Mg (++) , Si (++) , Al (+), S (+), K (tr), Fe(tr), P (tr)
CC9 finishing layer	Ca (+++), Mg (+++), Si (+), Al (tr), K (+), Fe(+), S (tr)
CC10 finishing layer	Ca (+++), Mg (+), Si (+), Al (+), K (+), Fe(+), S (tr)

Elements abundance: +++: very abundant; ++: abundant; +: present; tr: traces.

gypsum is present near lime in the finishing plaster whereas it is almost absent or just in traces in the underlying plasters.

The relevant height (more than 2 m from soil level) at which many plasters were sampled, the geological composition of the soil, and the location of the site in a Piedmont region not relevantly affected by air pollution discounted any external sulphate sources (such as capillary rise of sulphate-rich water or acid rain action). Moreover, while only gypsum crystals develop

in calcitic lime mortars, gypsum plus epsomite ($\text{MgSO}_4 \cdot 7\text{H}_2\text{O}$) and hexahydrate ($\text{MgSO}_4 \cdot 6\text{H}_2\text{O}$) crystallise in dolomitic lime mortars in the presence of particulate matter from diesel vehicle exhaust, one of the main pollutants in urban environments (Cultrone et al., 2008). None of these salts have been detected in our samples.

The above results support the use of mixed gypsum-lime mortars for most finishing layers used for the outside walls of the Chapel of Crucifixion. The use of these mixed mortars has

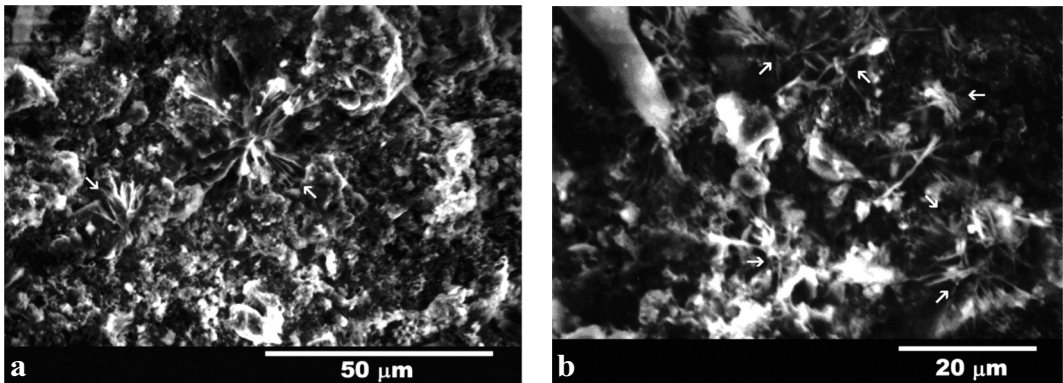


Figure 3. SEM micrograph of the finishing layer of sample CC5 a); higher magnification image of the acicular crystals merging from the finishing layer b).

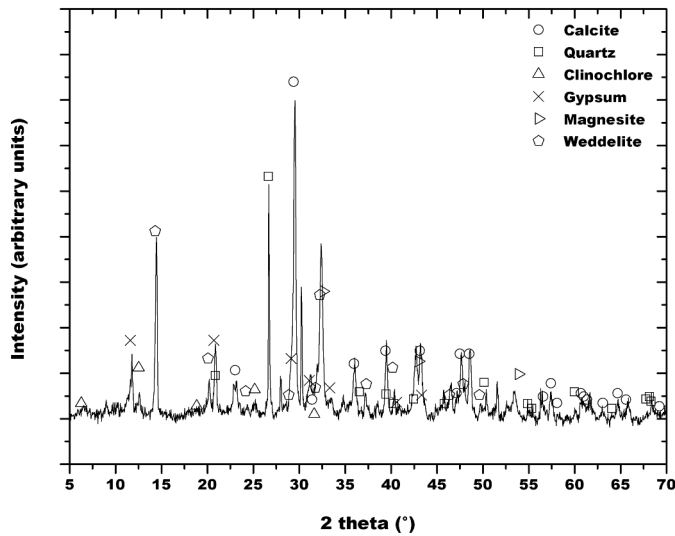


Figure 4. XRD pattern of the finishing layer of sample CC3.

been identified in many ancient buildings and decorative works and described in previous works (Genestar and Pons, 2003, Montana and Ronca, 2002).

From XRD analysis performed on the finishing layer, the presence of weddellite ($\text{CaC}_2\text{O}_4 \cdot 2\text{H}_2\text{O}$) in sample CC4 is probably the result of the interaction between organic matter and calcium carbonate, as noted by Montana and Ronca (Montana and Ronca, 2002).

From optical microscope observations, aggregates result of natural clasts with a grain size mostly in the field of the average-coarse sand (0.2-2 mm), and a significant amount of a finer fraction (0.06-0.2 mm) has been found only in all the samples (Figure 5, Table 3). Their sorting is from moderate to scarce and their roundness is low and is function of their mineralogical composition and of the transportation distance of each clast.

The clasts of greater size are formed by lithic fragments, while the fine-grained ones are mostly composed of single minerals. The

systematically and prevalent lithologies are siliceous rocks (gneisses, micaschists and quartzites), followed by greenschists and basic granulites; clasts of talcschists are relatively scarce but ubiquitous. Eclogites (absent in CC5 and CC7) are widespread, while ultramafics (samples CC1 and CC5) are more rare and kinzigites (sample CC1), serpentinites and marbles (sample CC10) have been only occasionally found (Table 4).

The gneissic lithologies are essentially represented by fine-grained gneisses made of quartz + albite \pm K-feldspar + clinozoisite + biotite and, subordinately, by orthogneisses (sample CC10) containing microcline porphyroclasts. The clasts formed by granolepidoblastic aggregates of quartz + white mica or lepidoblastic aggregates of white mica \pm sphene are referable to micaschists whereas to quartzites those formed by xenoblastic quartz only; these latter could also represent portions of micaschists and gneisses. The mineralogy of the clasts of greenschists is given by albite +

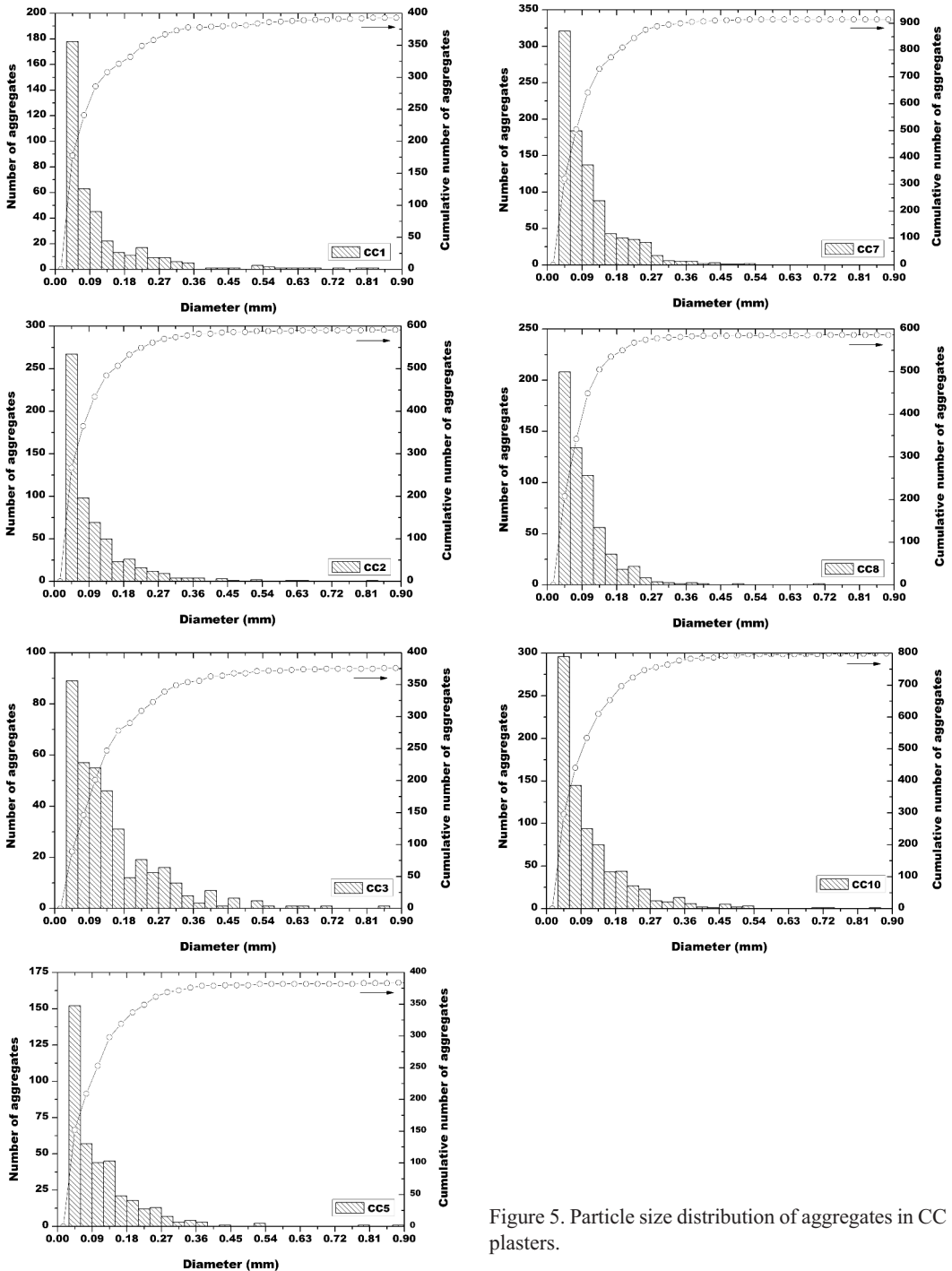


Figure 5. Particle size distribution of aggregates in CC plasters.

Table 3. Mean particle size, standard deviation and number of measured aggregates in CC plasters.

Sample	Number of aggregates	Mean diameter (mm)	Standard deviation (mm)	Minimum diameter (mm)	Maximum diameter (mm)
CC1	393	0.115	0.123	0.03	0.822
CC2	591	0.1	0.091	0.03	0.818
CC3	376	0.148	0.12	0.03	0.849
CC5	384	0.112	0.098	0.03	0.883
CC7	914	0.106	0.078	0.03	0.531
CC8	586	0.095	0.066	0.03	0.713
CC10	799	0.114	0.098	0.03	0.853

Table 4. Nature of the clasts found in the CC mortars.

Sample	CC1	CC2	CC3	CC5	CC7	CC8	CC10
<i>Lithic clasts</i>							
clinopyroxenite	+			+			
eclogite	+	+	+			+	
gneiss	++++	++++	++++	+++	+++	+++	++++
greenschist	+	+	+	+	+	+	++
kinzigite	+						
lherzolite	+						+
mafic granulite	+	+		+	++	++	
marble							+
serpentinite							+
<i>Mineral clasts</i>							
amphibole	++	++	++	++	+++	+++	++
biotite	++	++	+++	++	+++	+++	++
chlorite			+	+	+	+	+
clinozoisite/epidote	+		+++	+	+	+	+++
clinopyroxene	+	+	+	++	++	++	
garnet	++	++	++	+	++	++	+
K-feldspar			+				
olivine		+		+	+	+	
ores	++	++	+	+	+	+	+
plagioclase	+++	+++	++++	++++	++++	++++	++++
quartz	++++	++++	++++	++++	++++	++++	++++
sphene			+	+			+
talc							+
white mica	+	+	+	++	+	++	+++

The symbol + indicates the abundance (++++: very abundant; +++: abundant; ++: significant; +: present).

clinozoisite/epidote \pm green amphibole \pm chlorite \pm sphene; in the sample CC7 zoisite has been also observed. In the talcschists ore minerals are associated to the talc lepidoblasts. The clasts of basic granulites are constituted by polygonal granoblastic aggregates of plagioclase \pm clinopyroxene \pm brown amphibole \pm garnet \pm ores and those of eclogites by granoblastic aggregates of omphacite (mostly partly replaced by barroisitic amphibole + chlorite + white mica or by symplectite) \pm garnet \pm rutile \pm ores. Finally, the kinzigitic clasts can be easily distinguished from the other gneissic lithologies due to the presence of sillimanite \pm garnet (Table 4).

In the monomineralic clasts, additionally to the minerals listed above, olivine and also occasionally orthopyroxene and apatite have been found. Quartz and plagioclase are prevalent, always accompanied by biotite, white mica, brown amphibole, clinozoisite/epidote, chlorite, garnet and ores, among which pentlandite has been recognized in the sample CC10 by XRD analysis. The mineralogical-petrographical composition of the aggregates is quite homogeneous and easily referable to the alluvial deposits of the near Sesia River (Figure 6).

In all the samples the aggregate represents approximately 50% in volume of the plaster and the binder has always microcrystalline texture.

XRD analyses performed on the aggregate also support a common origin, since the results for each sample are very similar and mostly contain peaks of quartz (SiO_2), albite ($\text{NaAlSi}_3\text{O}_8$), lime (CaCO_3), muscovite $[(\text{K},\text{Na})(\text{Al},\text{Mg},\text{Fe})_2(\text{Si}_{3,1}\text{Al}_{0,9})\text{O}_{10}(\text{OH})_2]$ or $\text{KAl}_2(\text{Si}_3,\text{Al})\text{O}_{10}(\text{OH},\text{F})_2$, clinocllore $[(\text{Mg},\text{Fe},\text{Al})_6(\text{Si},\text{Al})_4\text{O}_{10}(\text{OH})_8]$, $[\text{Ca}_2(\text{Mg},\text{Fe}^{2+})_4\text{Al}(\text{Si}_7\text{Al})\text{O}_{22}(\text{OH},\text{F})_2]$, orthoclase $[(\text{K},\text{Ba},\text{Na})(\text{Si},\text{Al})_4\text{O}_8]$. In addition, samples CC2, CC7, CC9 contain clinozoisite $[\text{Ca}_2\text{Al}_3(\text{SiO}_4)(\text{Si}_2\text{O}_7)\text{O}(\text{OH})]$ and antigorite $[\text{Mg}_3\text{Si}_2\text{O}_5(\text{OH})_4]$. Finally, traces of talc $[\text{Mg}_3\text{Si}_4\text{O}_{10}(\text{OH})_2]$ were detected in sample CC5.

Square of the Courts

Certain variability in the nature of the plasters was evidenced comparing the materials sampled from different Chapels; SC1 from Chapel 24 is a typical lime mortar, whereas SC2 from Chapel 25, SC4 from Chapel 28 and SC5 from Chapel 29 are typical dolomitic lime mortars. The structure of the plaster SC6 from Chapel 29 is more complex because the finishing layer is a dolomitic lime mortar superposed on a common lime one.

Apart from samples SC1 and SC6, which present the same features as the samples from the complex of the Crucifixion, the plaster samples from the Square of the Courts show a clear stratification. Plaster SC6 presented a complex structure, but this could be due to sampling prior to thin-section preparation. In samples SC2, SC4 and SC5, the stratification is due to the nature of the aggregates, while in SC3 it is evidenced by the binder colour, in which an opaque substance, made of small grains, has been added (Figure 7). In samples SC2, SC4 and SC5, the second layer has a minor aggregate content but contains more carbonates (SC4) or is made quite exclusively of carbonates. Finally, in samples SC2 and SC5, carbonate clasts have an irregular shape, which suggests that they have been milled (Nowosielski et al., 2007).

In the binder of sample SC4 from Chapel 28 both pure magnesite (MgCO_3) and dolomite $[(\text{Ca},\text{Mg})\text{CO}_3]$ were detected by XRD (Figure 8) and confirmed by DSC-TG analysis (Figure 9). DSC curve presents 4 endothermic peaks at about 260°, 401°, 508° and 780 °C respectively, associated with mass losses of about 2.3, 6.7, 2.1 and 12.6%.

The endothermic effects at 258° and 408 °C are associated to the dehydration and dehydroxylation, respectively, of the hydromagnesite (Bruni et al., 1998), a magnesium carbonate hydroxide hydrate that forms in strictly controlled conditions, for example, when the solution pH ranges between

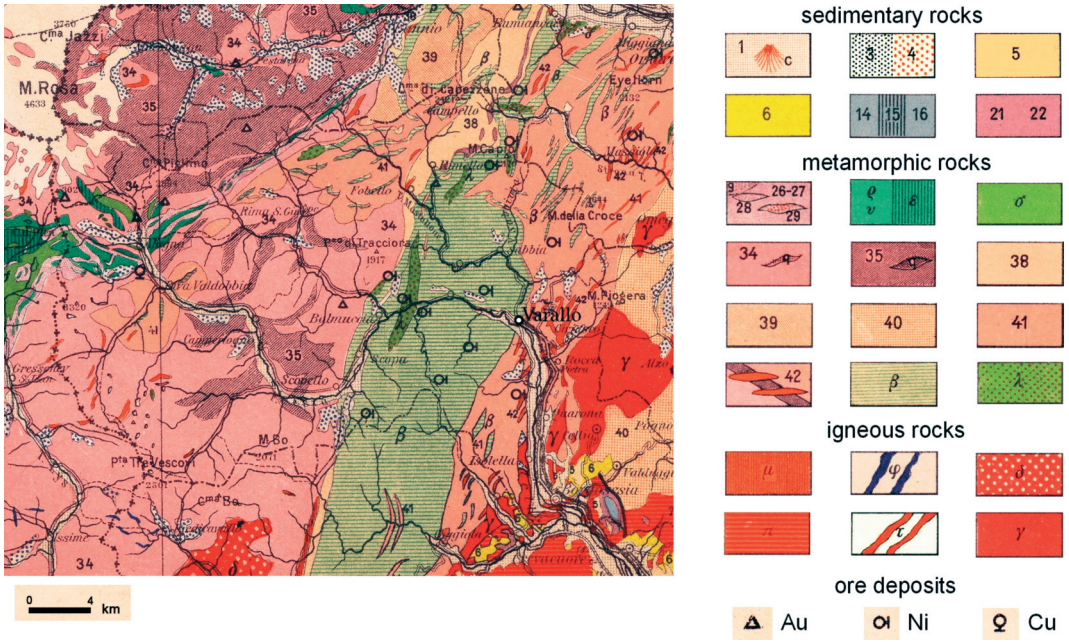


Figure 6. Lithological map of the catchment basin of the Sesia River in the Alpine area (from R. Ufficio Geologico, 1908, with changes in the legend).

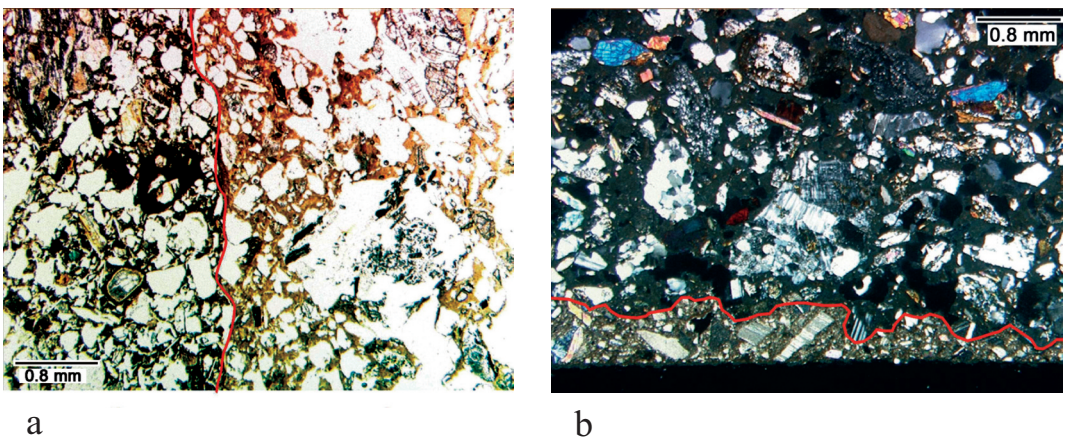


Figure 7. Cross sections of stratified samples (a) SC3 and (b) SC5.

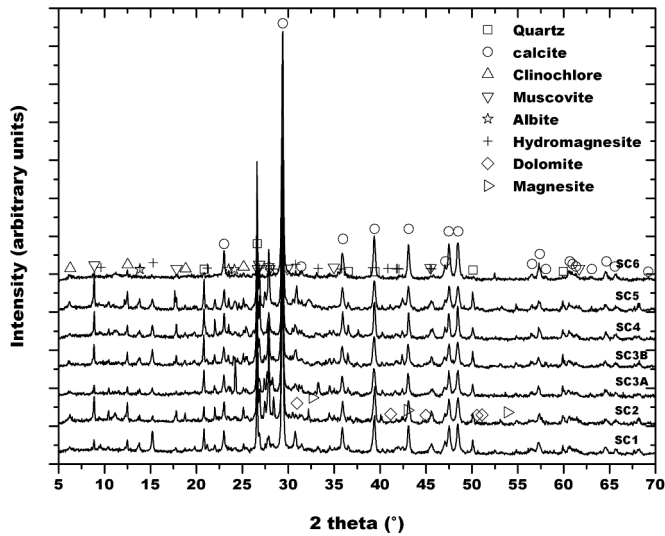


Figure 8. XRD pattern of the investigated SC plasters.

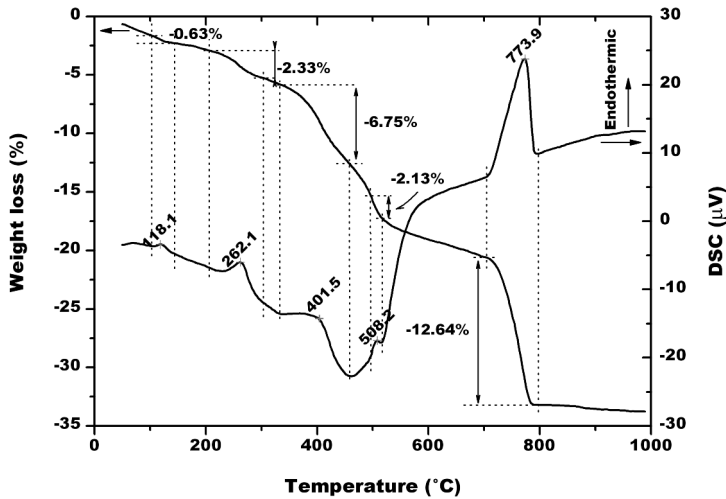
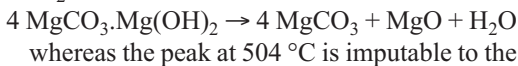
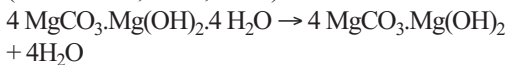


Figure 9. TG-DSC curve of sample SC4 from Chapel 28.

7.5 and 9.0 and in CO₂(g) excess conditions (Lanas et al., 2004, 2006).

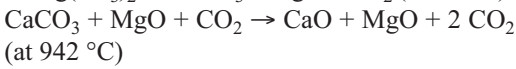
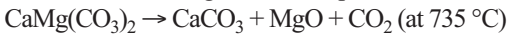


thermal decomposition of the magnesium carbonate, yielded by the previous reaction sequence:



Finally the broad peak centred at about 780 °C is due to the thermal decomposition of the

dolomite, following the two steps:



which are quite superposed in the adopted operative conditions (Fazeli and Tareen, 1992).

Several studies have shown that because of the particular lamellar structure of hydromagnesite, which confers a better homogeneity between the binder and the aggregates, the mortars present higher mechanical properties, in particular when exposed to humid environments as the site of the Sacro Monte of Varallo is (Hanchen and Prigibbe, 2008; Arizzi and Cultrone, 2012).

SC3 from Chapel 28 is particularly important among the many sampled from the Chapels of the Square of the Courts. This plaster presents a very

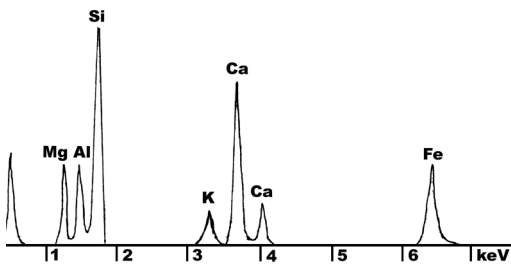


Figure 10. EDS analysis result on sample SC3 from Chapel 28.

complex structure: it is a white lime mortar with a finishing layer made of two parts, one having an almost black colour, about 3 mm thick, and then a thin surface layer, once again made of lime, rough and rich of coarse aggregate (Figure 7a).

The presence of iron detected in the finishing layer by EDS (Figure 10) suggests the addition of metallurgical slag rich in carbon residues (called “maciafer” in Piedmont), since its use as aggregate is known in the literature (Leslie et al., 2004; Hughes, 2006). To confirm this hypothesis, a sample of the dark portion was exposed to an oxidising flame and its colour changed to almost white; another part was immersed into a dilute chlorhydric acid solution: in addition to the typical effervescence due to the decomposition of the calcium carbonate, small carbonaceous particles were observed floating on the solution surface. Then, nitric acid was added to the solution, until the appearance of the typical yellow colour given by oxidation up to iron (III) ions. Charcoal is ubiquitous in historic mortars but its presence, as a pigment added to darken the mortar, has been already reported (Hughes, 2006).

Elemental composition analyses performed on the finishing layers by EDS (Table 5) revealed

Table 5. EDS analysis results on SC samples.

Sample	Elements
SC1 finishing layer	Ca (+++), Mg (+), Si (+), Al (tr), K (tr), Fe (tr)
SC2 finishing layer	Mg (+++), Ca (+), S (tr), Si (tr), Al (tr), Fe (tr), K (tr)
SC3 finishing layer	Si (+++), Mg (+), Al (+), Ca (+), Fe (tr), K (tr)
SC4 finishing layer	Mg (+++), Ca (++), Si (++), Fe(+), S (tr), Al (tr), K (tr), Fe (tr),
SC5 finishing layer	Ca (+++), Mg (+), Si (tr), Al (tr), K (tr), Fe(tr)
SC6 finishing layer	Mg (+++), Ca (+), Si (tr), Al (tr), K (tr), Fe (tr)

Elements abundance: +++: very abundant; ++: abundant; +: present; tr: traces.

Table 6. Nature of the clasts found in the SC mortars.

Sample	SC1	SC2A	SC2B	SC3A	SC3B	SC4A	SC4b	SC5A	SC5B	SC6
<i>Lithic clasts</i>										
clinopyroxenite						+	+			
eclogite				+	+					
gneiss	++	+++		++	++	++	++	++		+++
greenschist	+	++		+	+	+	+	+		
kinzigite	+									+
mafic granulite	+	+		+	+	+	+	+	+	+
mica schist/quartzite	+++	+++		+++	+++	+++	+++	+++		++
serpentine	+	+								
<i>Mineral clasts</i>										
amphibole	+	+			+	+	+	+		+
biotite	++	+			+	+	+	+		+
calcite/dolomite			++++				++++		++++	
chlorite		+			+	+	+	+		+
clinzoisite/epidote		+		+		+	+	+		+
clinopyroxene	+	+		+				+		+
garnet	+	+				+	+	+		+
gypsum			+	(?)					+	
K-feldspar	+	++		+				+		
olivine						+	+			
ores	+	+	+	+		+	+	+		+
plagioclase	++	++			++	+	+	+		++
quartz	+++	+++	+		+++	++	++	++		++
talc	+	+		+		+	+	+		+
white mica	+	+			+	+	+	+		+

The symbol + indicates the abundance (++++: very abundant; +++: abundant; ++: significant; +: present).

that samples SC2, SC4 and SC6 have magnesium-rich upper layers.

Optical microscope observations of the SC samples showed compositions (Table 6) and characters (Figure 11, Table 7) very similar to those of the Chapel of the Crucifixion (Table 4) and the aggregates generally ranged from more than 40% in volume of the plaster up to about 70% in sample SC3. Their size lie mostly in the field of the average-coarse sand (0.2-2 mm). Samples SC3, SC4 and SC5 presented a complex structure made of a finishing layer constituted of two parts labelled A and B (Table 6). The

mineralogical-petrographical composition of these aggregates are quite homogeneous and easily referable to the alluvial deposits of the near Sesia River (Figure 6).

Chapel of the Mount Tabor

As for the materials sampled from the Chapels of the Square of the Courts, a certain variability in the nature of the plasters from the Chapel of the Mount Tabor was evidenced by comparing the materials sampled from different points of the Chapels.

Optical microscope observations of the

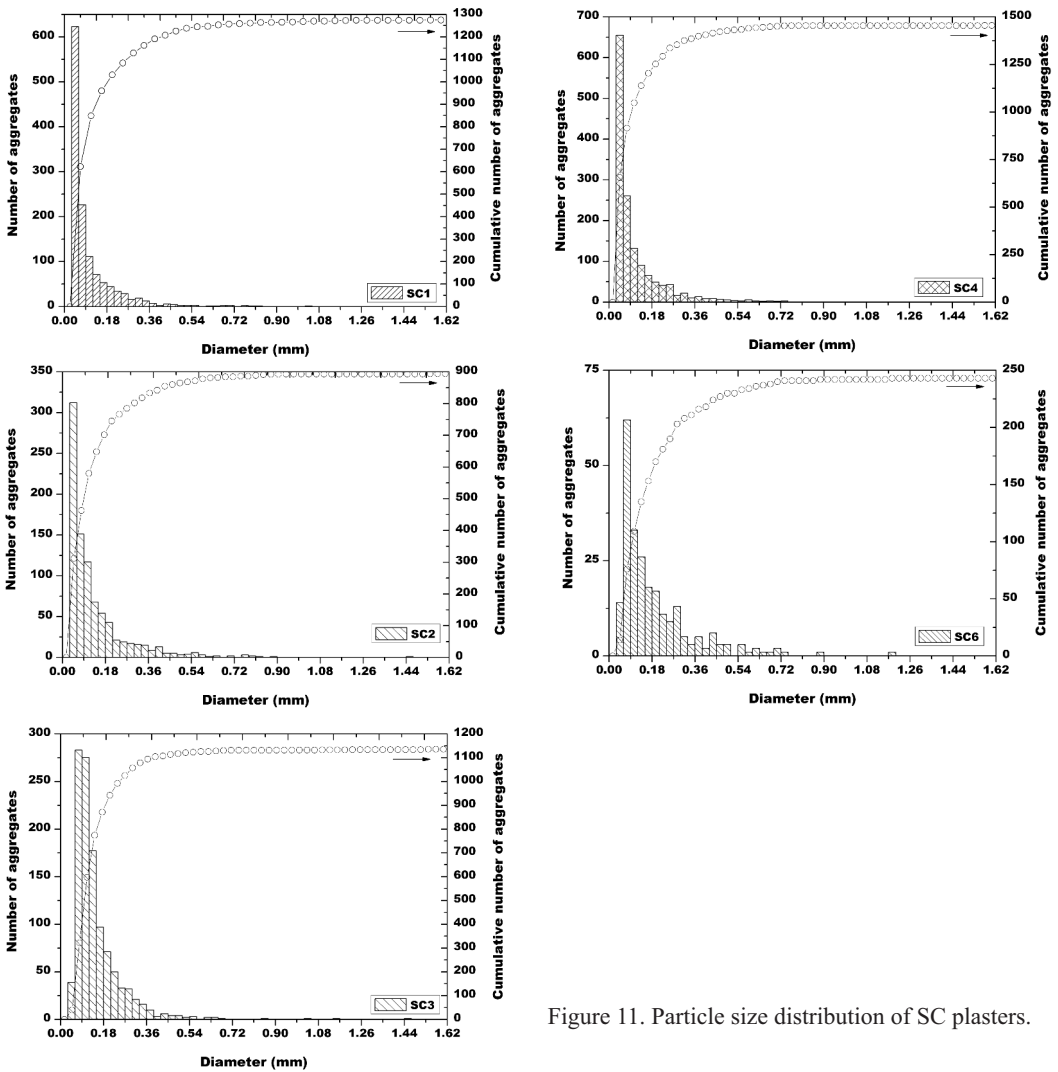


Figure 11. Particle size distribution of SC plasters.

Table 7. Mean particle size, standard deviation and number of measured aggregates in SC plasters.

Sample	Number of aggregates	Mean diameter (mm)	Standard deviation (mm)	Minimum diameter (mm)	Maximum diameter (mm)
SC1	1275	0.102	0.106	0.03	1.05
SC2	894	0.134	0.138	0.03	1.451
SC3	1135	0.149	0.108	0.03	1.469
SC4	1455	0.112	0.12	0.03	1.569
SC6	243	0.192	0.164	0.03	1.172

samples MT1, MT2 and MT4 show compositions (Table 8) and characters (Figure 12, Table 9) very similar to those of the Chapel of the Crucifixion, though the aggregates generally represent more than 50% in volume of the plaster and reach about 70% in MT1. The main lithologies are still siliceous rocks (micaschists and fine-grained gneisses), but associated with abundant marble; furthermore in the monomineralic clasts the calcite is prevailing in comparison to the silicates (quartz, albite, K-feldspar, clinozoisite, white mica and biotite).

This composition is compatible with the alluvial deposits of the Sorba Stream, tributary of the Sesia River and whose confluence with this is located about 20 km from Varallo (Figure 6).

Under the microscope the aggregates result of natural clasts with a grain size mostly in the field of the average-coarse sand (0.2-2 mm) (Figure 12).

The siliceous clasts are generally angular whereas the carbonatic ones are subrounded, and the aggregate represents approximately 40% in volume of the plaster.

MT2 is a typical lime mortar, whereas MT1

Table 8. Nature of the clasts found in the MT mortars.

Sample	MT1	MT2	MT3	MT4
<i>Lithic clasts</i>				
clinopyroxenite	+	+		
eclogite		+		+
gneiss	++	++	+	+++
greenschist	+			
kinzigite				
mafic granulite		+		+
mica schist/quartzite	++++	++++	+	++
serpentinite		+		+
<i>Mineral clasts</i>				
amphibole				
biotite	+			+
calcite/dolomite			++++	
chlorite	+	+		+
clinozoisite/epidote	+	+	+	+
clinopyroxene	+	+		+
garnet	+			+
gypsum				
K-feldspar	+	+	+	
olivine				
ores				
plagioclase	++	+	+	+
quartz	++++	+++	+	+++
talc	+	+		
white mica		+	+	++

The symbol + indicates the abundance (++++: very abundant; +++: abundant; ++: significant; +: present).

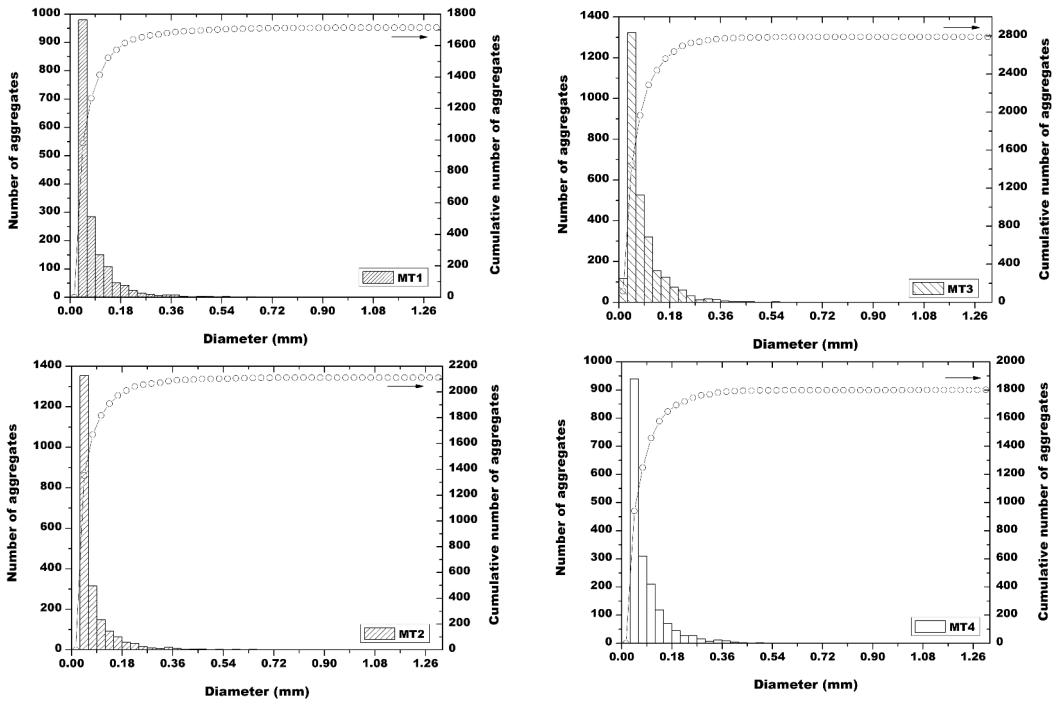


Figure 12. Particle size distribution of MT plasters.

Table 9. Mean particle size, standard deviation and number of measured aggregates in MT plasters.

Sample	Number of aggergates	Mean diameter (mm)	Standard deviation (mm)	Minimum diameter (mm)	Maximum diameter (mm)
MT1	1715	0.084	0.09	0.03	1.227
MT2	2113	0.076	0.113	0.03	3.017
MT3	2790	0.083	0.067	0.03	0.701
MT4	1802	0.085	0.079	0.03	1.307

presents a more complex structure in which the finishing layer is a dolomitic lime mortar superposed on a common lime one (Figure 13) (Table 10).

A double layered structure was also observed in the case of sample MT4, but in this case a lime-

gypsum finishing layer was observed on the common lime mortar, similar to many materials sampled from the Chapel of the Crucifixion (Figure 14).

Finally, the sample MT3 presented another compositional feature; this plaster is made of a

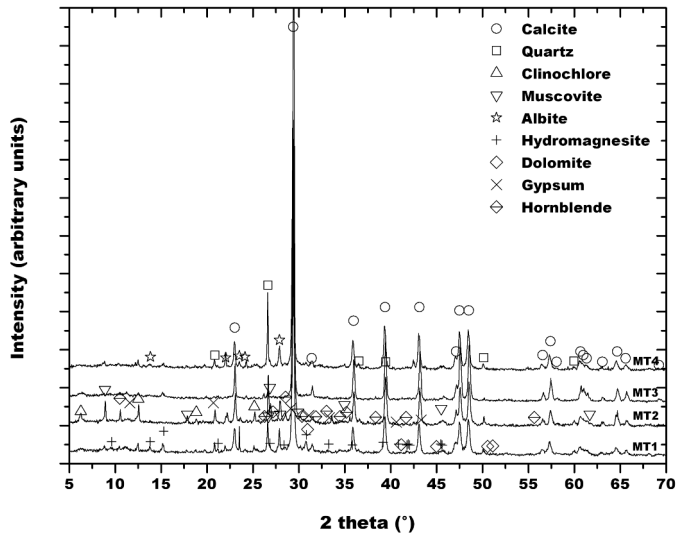


Fig 13. XRD pattern of the investigated MT plasters.

Table 10. EDS analysis results on MT samples.

Sample	Elements
MT1 finishing layer	Mg (+++), Ca (tr), Si (tr), Al (tr), S (tr)
MT2 finishing layer	Ca (+++), Mg (tr), Si (tr), Al (tr), Fe (tr), K (tr)
MT3 finishing layer	Ca (+++), Mg (tr), Si (tr), Al (tr), K (tr)
MT4 finishing layer	Ca (+++), S (+++), Si (tr), Al (tr), K (tr)

Elements abundance: +++: very abundant; ++: abundant; +: present; tr: traces.

lime binder in which fine and coarse angular aggregates merge from the surface of the finishing layer (Figure 15). EDS as well as petrographic and XRD analyses (Figures 16-17) confirmed that this plaster is made of a lime binder in which fine and coarse marble particles are dispersed as aggregates. The use of angular fragments of white marble as sand in snow-white finishing layers is already witnessed in stucco works (Montana and Ronca, 2002) and it was probably exploited in this case to create a particular finishing effect.

Conclusions

Results from the 20 investigated plasters coming from 3 different relevant buildings of the “Sacro Monte” indicated that in all cases aerial binders, based on calcite, dolomite, or a mixture of both, were used together with local aggregates from the Sesia River. In various cases (the samples coming from the Chapel of the Crucifixion), gypsum was present in the finishing layer, while almost absent in the

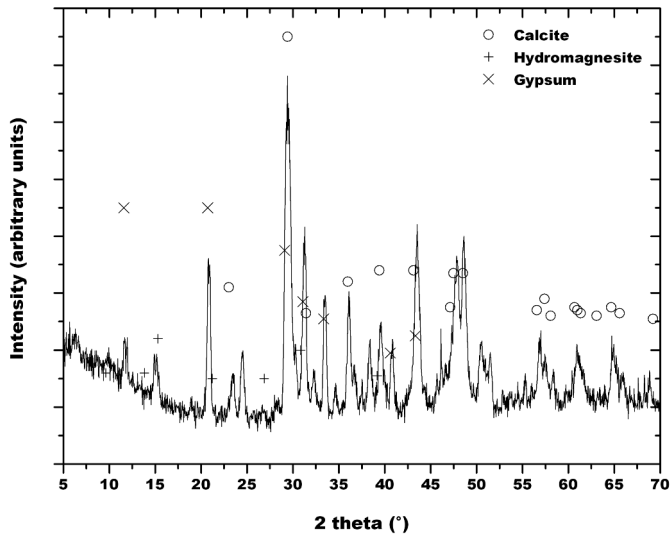


Fig 14. XRD pattern of the upper surface of sample MT4.

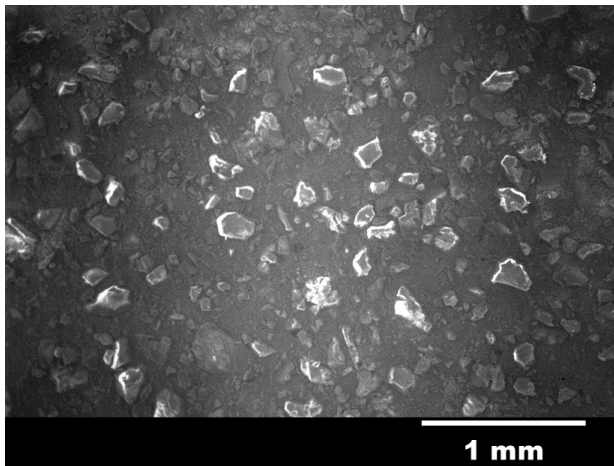


Fig 15. SEM image of the upper surface of sample MT3.

underlying layers, as reported in the literature. Structured layers were observed in Mount Tabor and Square of the Courts structures, probably in order to obtain particular finishing effects: a dark layer after additions of iron-rich metallurgical

slags (sample SC3) and a snow-white finishing layer, similar to a stucco work for sample MT3.

These chemical characterization of mortars have provided useful knowledge as regards the ancient building materials: thanks to these results, it will be

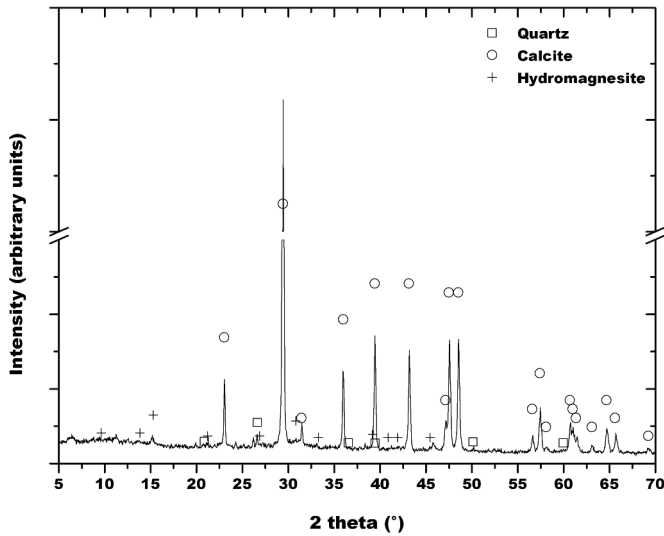


Fig 16. XRD analysis results on the sample MT3 sieved at 45 microns.

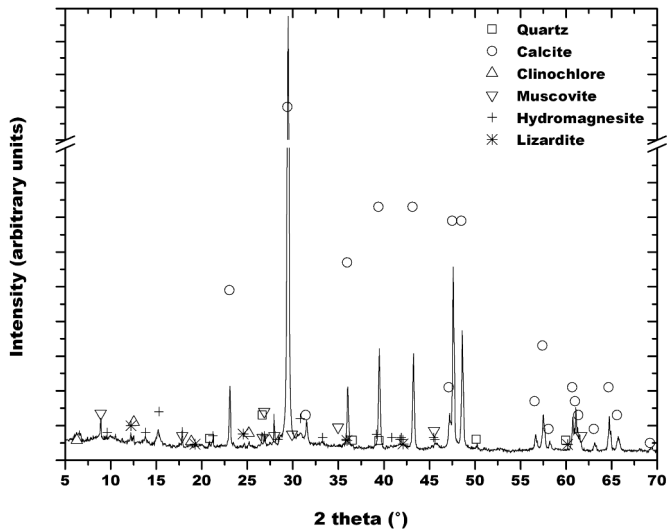


Fig 17. XRD analysis results on the sample MT3 sieved at 600 microns.

possible, for instance, to prepare restoration mixture having characteristics compatible with the masonry structure, through a ‘reverse engineering’ process. This is of particular importance as, for example, the combination of sulphate and magnesium-bearing

mortars and stone with high magnesium content is known to be problematic, due to the possible formation of deleterious magnesium sulphates salts, and thus should be avoided in restoration works (Lopez-Arce et al., 2009).

Acknowledgements

The authors wish to thank the shop “Immagini e Computer” (Dr. Abbate and Mrs Barlottini) in Bareggio (Milano), Italy for the possibility of using an evaluation version of the software Image-Pro Plus to perform image analysis on the plasters cross-sections. Two anonymous referees are acknowledged for improving the manuscript.

References

- AA.VV. (1514) - Questi sono li Misteri che sono sopra el Monte de Varalle. In: Stefani Perrone S (ed) (1987) Guida poetica del 1514, Borgosesia.
- AA.VV. (1842) - Archivio storico di Varallo, Fondo Sacro Monte, B 65.
- Arizzi, A. and Cultrone G. (2012) - The difference in behaviour between calcitic and dolomitic lime mortars set under dry conditions: The relationship between textural and physical-mechanical properties. *Cement and Concrete Research*, 42, 6, 818-826.
- Callebaut K., Elsen J., van Balen K. and Viaene W. (1999) - Historical and scientific study of hydraulic mortars from the 19th century, in International RILEM Workshop on Historic Mortars: Characteristics and Tests, P. Bartos, C. Groot and J. J. Hughes Editors, 125-132.
- Bruni S., Cariati F., Fermo P., Pozzi A. and Toniolo L. (1998) - Characterization of ancient magnesian mortars from northern Italy. *Thermochimica Acta*, 321, 161-165.
- Cultrone G., Arizzi A., Sebastián E. and Rodriguez-Navarro C. (2008) - Sulfation of calcitic and dolomitic lime mortars in the presence of diesel particulate matter. *Environmental geology*, 56, 741-752.
- Elsen J. (2006) - Microscopy of historic mortars - a review. *Cement and Concrete Research*, 36, 1416-1424.
- Fazeli A.R. and Tareen J.A.K. (1992) - Thermal decomposition of rhombohedral double carbonates of dolomite type. *Journal of Thermal Analysis and Calorimetry*, 38, 2459-2465.
- Galí S., Ayora C., Alonso P., Tauler E. And Labrador M. (2001) - Kinetics of dolomite -portlandite reaction Application to Portland cement concrete. *Cement and Concrete Research*, 31, 933-939.
- Galloni P. (1914) - Sacro Monte di Varallo. Origine e svolgimento delle opere d'arte. Varallo
- Genestar C. and Pons C. (2003) - Ancient covering plaster mortars from several convents and Islamic and Gothic palaces in Palma de Mallorca (Spain). Analytical characterization. *Journal of Cultural Heritage*, 4, 291-298.
- Hanchen M. and Prigiobbe V. (2008) - Precipitation in the Mg-carbonate system-effects of temperature and CO₂ pressure. *Chemical Engineering Science*, 63a, 1012-1028.
- Lanas J. and Alvarez J.I. (2004) - Dolomitic limes: evolution of the slaking process under different conditions. *Thermochimica Acta*, 423, 1-12.
- Lanas J., Pérez Bernal J.L., Bello M.A. and Alvarez J.I. (2006) - Mechanical properties of masonry repair dolomitic lime-based mortars. *Cement and Concrete Research*, 36, 951-960.
- Leslie A.B. and Hughes J.J. (2004) - High-temperature slag formation in historic Scottish mortars: evidence for production dynamics in 18th-19th century lime production from Charlestown, *Materials Characterization*, 53, 181-186.
- Lopez-Arce P., Garcia-Guinea J., Benavente D., Tormo L. and Doehne E. (2009) - Deterioration of dolostone by magnesium sulphate salt: An example of incompatible building materials at Bonaval Monastery, Spain. *Construction and Building Materials*, 23, 846-855.
- Montana G. and Ronca F. (2002) - The “recipe” of the stucco sculptures of Giacomo Serpotta. *Journal of Cultural Heritage*, 3, 133-145.
- Nowosielski R., Babilas R., Dercz G., Paj L. and Wrona J. (2007) - Structure and properties of barium ferrite powders prepared by milling and annealing. *Archives of Materials Science and Engineering*, 28, 12, 735-742.
- Stefani Perrone S. (1984) - Il Sacro Monte di Varallo. In: Monumenti di fede e di arte in Varallo. Borgosesia.
- Stefani Perrone S. (1994) - Guida al Sacro Monte di Varallo. Turin, Proget s.r.l, Kosmos Edizioni.

Submitted, August 2012 - Accepted, April 2013